Journal of Environmental Monitoring

Cite this: *J. Environ. Monit.*, 2012, **14**, 3295

www.rsc.org/jem

PAPER

Field-deployable and near-real-time optical microfluidic biosensors for single-oocyst-level detection of *Cryptosporidium parvum* from field water samples

Scott V. Angus, Hyuck-Jin Kwon and Jeong-Yeol Yoon*

Received 22nd August 2012, Accepted 24th October 2012
DOI: 10.1039/c2em30700f

Cryptosporidium spp. is an obligate, parasitic protozoan that is difficult to detect and causes diarrhea in healthy adults while potentially causing death in the immunocompromised and children. Its treatment options are few and treat the symptoms, not the actual parasite. Current methods of detection are inefficient and rely too heavily upon laboratory sample preparations and technician skill, including differential staining, negative staining, and immunofluorescence methods [especially U.S. Environmental Protection Agency (EPA) Method 1623]. These assays can take from hours to days and require a laboratory environment. In this work, we demonstrated the microbead immunoagglutination assay combined with Mie scatter detection in a microfluidic device to provide a field-deployable and near-real-time alternative to the laboratory-based method (especially EPA Method 1623). Two main challenges were the relatively big diameter of *Cryptosporidium* oocysts (5–6 μm) and the contaminants in field water samples that negatively affected the immunoagglutination and its scatter detection. We used 4 min sonication to liberate *Cryptosporidium* oocyst wall proteins (COWP), which was previously used to inactivate *Cryptosporidium* oocysts. As for the contaminants, we optimized the microbead diameter (920 nm) and the wavelength of incident light (375 nm) to find the angle of scatter detection (45°) where the Mie scatter from immunoagglutinated microbeads was maximum and the background scatter from contaminants was minimum. This enabled the sub-single-oocyst-level detection despite the fact that only a very small volume of water sample (15 μL) was introduced to the microfluidic biosensor. When combined with filtration/concentration, this method is able to detect ≤1 oocyst per large volume of water, comparable to or potentially better than the EPA method 1623, while effectively reducing the time and labor necessary for staining and microscopic analysis. For faster, near-real-time assays, filtration/concentration may not be used, where the detection limit was 1–10 oocysts per mL with the total assay time of 10 min including the 4 min sonication time. The linear range of assay was over 5 orders of magnitude. The final device was compact and had the potential to be used in field situations, and required less technical expertise and/or training compared to the other methods.

Introduction

Cryptosporidium spp. are a group of obligate, intracellular, parasitic protozoa first discovered and described by Tyzzer in 1907 and found to be pathogenic to humans by Nime *et al.* and Meisel *et al.* in 1976 in immunocompromised individuals.[1] While healthy individuals have little to worry about concerning

Department of Agricultural and Biosystems Engineering, The University of Arizona, Tucson, Arizona 85721-0038, USA. E-mail: jyyoon@email.arizona.edu; Fax: +1-520-621-3963; Tel: +1-520-621-3587

Environmental impact

Cryptosporidium is increasingly a concern for municipal water supplies worldwide as standard methods of water treatment are simply ineffective in killing the hardy protozoan oocysts. It is very difficult to detect it currently with many cases likely going unreported as symptoms are very general, typically involving dysentery and dehydration. It can be found readily in the environment as UV exposure will not kill the oocysts. The current detection methods require upwards of ten liters of water, a concentration process, and difficult laboratory based testing. We propose a new method that is faster, more environmentally sound, and more effective in finding this hardy, difficult to detect protozoan parasite.

Cryptosporidium infections, other than minor discomfort for one to several weeks, children, immunocompromised individuals, and those in close or constant contact with young children are at a high risk and the illness can last for months.[2] Symptomatically, *Cryptosporidium* causes mild to severe diarrhea, dehydration, stomach cramps, and possibly a slight fever.[1] This is known as cryptosporidiosis. It is typically contained in the lower intestines, but in immunocompromised individuals (such as those with acquired immune deficiency syndrome —AIDS— and those undergoing chemotherapy treatments) and children, it can spread to other areas of the body. It has a documented infectious dose in 50% of the experimental group (ID_{50}) ranging from 9–1024 oocysts[2] with reports also estimating it at 83–123 oocysts[3] and clinical reports (defined as diarrhea but no shedding of oocysts) ranging from 10–83 oocysts per individual.[3] It can be very difficult to treat as it is located intracellularly but extracytoplasmicly.[4] Most treatment methods rely on treating the symptoms, such as dehydration and diarrhea. It is estimated that the mortality rate for immunocompromised individuals is as high as 50%.[5]

There are two primary species that are infectious to humans: *C. parvum* and *C. hominis* (formerly *C. parvum* genotype 1). *Cryptosporidium* oocysts follow a fecal-oral route to initiate infection of a new host, making it easy for infections to spread. Oocysts can survive easily in the environment and are found especially near agricultural areas.[6] Castro-Hermida *et al.* described levels of *Cryptosporidium* 5 to 3375 times higher near agricultural areas in surface water sources.[6] When *Cryptosporidium* outbreaks occur, they are often traced back to a municipal water supply's deficiencies or contamination. However, it can be found in food, contaminated water, and, most commonly, in fecal matter.[7] Standard methods for sterilizing drinking water will kill most everything in fecal matter, but *Cryptosporidium* is highly resistant to many, if not all of these methods, as oocysts have been found in water treatment facilities' effluent at a rate of up to 75%.[8]

Due to the resilient nature of the oocyst, chlorine is nearly completely ineffective, even though it is a primary means for modern chemical water cleaning, especially in swimming pools. To kill *Cryptosporidium*, 80 ppm of chlorine is required, while swimming pools typically have only 3–4 ppm chlorine.[9] It has been suggested that swimming pools should have separate water reservoirs, filtration systems, and treatment systems for the shallow "kiddie" swimming pools, in addition to the systems that treat mainly the adult sections of the pool.[2]

Between 1984 and 1999, there were an estimated 54 outbreaks attributable to *Cryptosporidium* spp., in developed nations, with at least 421 000 individual cases.[7] This accounts for 73% of all waterborne outbreak cases involving drinking water.[10] In the U.S. Environmental Protection Agency's (EPA) National Primary Drinking Water Regulations: Long Term 2 Enhanced Surface Water Treatment Rule (LT2ESWTR), it is stated that the number of cases reported to the U.S. Centers for Disease Control (CDC) is likely a gross underestimate.[3] It is documented, based on interpolation, that there are likely at least 300 000 cases annually, many of which are endemic, isolated, and unreported.[1,3,7] In the LT2ESWTR, the minimum concentration of oocysts in influent water supply at a water treatment plant (WTP) that requires no special treatment is 0.075 oocysts per L. Anything above this requires additional treatment methods, requiring up to a 3-log treatment.[1]

Poor diagnostic methods as well as a poor understanding of the pathogen by the general public and physicians[1] have undoubtedly led to higher numbers of infection and worse treatment. The current EPA-approved detection method, Method 1623, requires a minimum of 10 liters of water, but due to concentration and sample quality requirements, more can easily be required.[11] The method is expensive and difficult to run. It requires a trained technician with expensive microscopic and filtration equipment, dyes, and reagents. The microscopic equipment and technicians must be tested on a monthly basis for accuracy and calibration. The method requires three visual examination steps, introducing further steps where error and subjectivity can be/are injected into a scientific method. The method also has problems with false positives due to autofluorescence of algae and yeast biomaterial.[11] Though this method is validated and accepted for environmental samples, it is inefficient, extremely complicated, and not applicable in (near-real-time) field testing.

In addition to the EPA-approved Method 1623, many other methods have been tested to detect *Cryptosporidium* spp. from water and fecal samples, as summarized in Table 1. They were categorized into three groups: staining-based, antibody-based, and nucleic acid-based. The detection limits of staining methods are typically in the order of 10^1 to 10^3 oocysts per a few tens or hundreds of μL water sample or per g fecal sample, roughly equivalent to 10^2 to 10^5 oocysts per mL. Detection limits of antibody-based methods are better, typically in the order of 1–10^3 oocysts per mL water or per g fecal sample. While EPA Method 1623 showed the lowest detection limit, it is actually the most complicated and time consuming assay. Almost all methods require filtration and/or concentration, similar to Method 1623.

Polymerase chain reaction (PCR) is typically a gold standard for detecting a specific target in a biologically active sample; however, there have been problems with this in the past. Two primary sequences used are the *Cryptosporidium* oocyst wall protein (COWP) gene and 18S rRNA gene. In one study, samples have been so contaminated that as few as 6 samples had successful PCR assays performed out of a total of 16 samples.[8] There have been other problems as well, such as different species being found in the influent and effluent after performing PCR assay,[12] indicating false positives and false negatives. It has also been noted that genetic diversity exists within *Cryptosporidium* spp. as they are identified today.[13] This has undoubtedly led to problems in identification of *Cryptosporidium* spp. in clinical and other settings. PCR-RFLP (PCR-restriction fragment length polymorphism) has shown promise,[14] but is still restricted by the speeds of conventional PCR.

The main objective of this work is to demonstrate a field-deployable and near-real-time assay for detecting *Cryptosporidium* oocysts from field water samples, with a reasonable detection limit, as a field-applicable alternative or an improvement to the laboratory based Method 1623. We demonstrate the microbead immunoagglutination assay combined with Mie scatter detection in a microfluidic device to meet the field-deployable and near-real-time requirements. Since this particular method has been demonstrated to show the improvement in detection limit by several orders of magnitude compared to the

Table 1 Literature survey of detection methods for *Cryptosporidium* spp[a]

Method	Detection limit	Filtration	Concentration	Assay time	Sensitivity Specificity	Sample matrix	Ref.
Staining Based							
Modified Ziehl–Neelsen (acid fast)	1 oocyst per 100 μL	No[28,29] Not reported[30]	Yes (formalin–ethyl acetate)	45 min to overnight	89% 100%	Fecal	28–30
Auramine–rhodamine	9–205 oocysts per 3 in^2 slide	No	No	45 min+	93.8% 100%	Fecal	31 and 32
DMSO–carbol-fuchsin	Not reported	Not required	Yes (not necessary)	30 min w/o concentration	High Low	Fecal	33
Flow cytometry	10 to 5×10^4 oocysts per g feces	Yes	Yes (centrifuge, flocculate, dilute)	90 min to >12 h	81.3–100% 87–100%	Surface water, WTP effluent, stool	34–38
Kinyoun	>275 oocysts per 10 μL	No	Yes (centrifuge, flocculate, dilute)	2 h	96% 97–100%	Stool	39 and 40
Light green merbromide	Not reported	Not reported	Yes (lyse)	2–3 h	66–100% 100%	Fecal (dilute)	41
Malachite green	10^2 oocysts per g	No	Yes (centrifuge)	25 min	0–17.2%	Fecal	42
Safranin–methylene blue stain	Not reported	Yes (zinc sulphate flotation)	No (dilute if necessary)	>30 min	86% 90.9–100%	Fecal	42–45
Surface enhanced Raman	1000 oocysts per 20 μL	No (spiked samples only)	No (spiked samples)	>3 h	100% 85%	Purified oocysts	46
Antibody based							
Dot blotting w/mAbs	10^2 oocysts per g	No (spiked samples only)	Yes (centrifuge)	>15 min	Not reported	Fecal	47
ELISA	10^3 to 3×10^5 oocysts per L	Yes	Yes (centrifuge, sonicate)	90–250 min	82.3–100% 96.7%	Fecal	39,48–54
Immunofluorescence w/mAbs	1 oocyst per 10 μL	Not required	Yes (centrifuge, FEA)	10–90 min	93–100% 100%	Fecal	29,31,37,55–58
Immunofluorescence microscopy (Method 1623)	0.25–0.4 oocysts per L	Yes	Yes	>3 h	2–83% 93–100%	Natural water, WTP effluent,	6,8,59–63
Immunomagnetic electro-chemiluminescence	5 oocysts per mL	Yes (decanting)	Yes (centrifuge multiple times)	>5 h	11–24% Not reported	surface water	64
Latex agglutination	Not reported (yes/no only)	Yes	Not reported	Not reported	Not reported	Fecal	65
Polyclonal fluorescent antibody test	21–210 oocysts per 3 in^2 slide	Yes	Yes (centrifuge)	>90 min	High Very high	Manure	32
Reverse passive haemagglutination	Not reported	Yes	Yes (dilution required)	>2 h	93.9% 98.2%	Fecal	66
Solid-phase immuno-chromatographic assay	Not reported	No	No	10–20 min	97.56% 100%	Fecal	67
Nucleic acid based							
AFLP (amplified fragment length polymorphism) PCR	10–15 ng DNA per 50 μL	Yes (oocyst/ DNA purification)	Yes (centrifuge multiple times)	2–4 h	Very high	Purified oocysts	68
Fluorescent *in situ* hybridization (FISH)	1–150 oocysts per 2–4 g feces	Yes (cellulose membrane)	Yes (centrifuge)	1–24 h	Very high 100%	Oyster, fecal	69 and 70
PCR	1–10^6 oocysts per sample	Yes (oocyst purification)	Yes (centrifuge multiple times)	1–48 h	84.7–97.2% 100%	Fecal, water, milk, purified oocysts	71–76
PCR-RFLP (restriction fragment length polymorphism)	100–500 oocysts per fecal sample	Not reported	Yes (centrifuge)	2–4 h	94% Low	Fecal	77–79

[a] Note: DMSO = dimethyl sulfoxide; ELISA = enzyme-linked immunosorbent assay; mAb = monoclonal antibody; PCR = polymerase chain reaction; WTP = water treatment plant.

other immunoassays,[15,16] it should demonstrate the same low detection limit as that of Method 1623 when used together with filtration and/or concentration.

There exist a number of challenges in detecting *Cryptosporidium* oocysts using a microbead immunoagglutination assay with Mie scatter detection in a microfluidic device. The first challenge is the size of *Cryptosporidium* oocysts. At 5–6 μm in diameter,[17] it is significantly larger than bacteria and viruses as well as the typical submicron beads used in immunoagglutination assays. The submicron, antibody-conjugated polystyrene beads must form doublets or triplets, so that the effective bead diameter can increase. This increase in effective diameter can be detected by Mie scatter at a certain scattering angle, as it is dependent more on the bead diameter and scattering angle, while less on the wavelength of incident light and microbead concentration. Since the oocysts are much larger than the antibody-conjugated microbeads, the immunoagglutinated beads will not be seen as a single entity but rather separate beads. In addition, the necessary diffusion of oocysts towards the antibody-conjugated beads is limited by their large diameter, which will significantly limit the extent of immunoagglutination. Therefore, it is necessary to break off the surface antigens from the oocysts to facilitate the immunoagglutination. Since the oocysts are relatively big, sufficient number of antigens can be generated and sub-single-oocyst-level detection may become possible.

Sonication has been considered as a viable, yet rapid method for inactivation of *Cryptosporidium* oocysts. After approximately 5.2 minutes, only 20% of oocysts have an intact oocyst wall and 97% are inactivated.[18] Through sonication, the *Cryptosporidium* oocyst wall protein (COWP) or other internal structures can be broken apart and become available for binding with antibodies. Since sonication is effective and rapid in breaking off COWP, we use this method to facilitate microbead immunoagglutination assays in a microfluidic platform.

The second challenge is the turbidity of the field water sample (the same can be applied to the fecal sample dissolved in buffer). Since our method utilizes light scattering detection, any turbidity from the sample matrix can compromise the light scattering signal. In scatter theory, the refractive index (n) is an important parameter that determines the strength of scatter signals. For the UV wavelength (375 nm) used in this study, $n = 1.34$ for water, while $n = 1.62$ for polystyrene beads, which are substantially different from each other.[19] For typical proteins, $n = 1.38$–1.40, close to that of water.[15] Most turbidity from field water originates from silica or clay particles. For silica, $n = 1.56$ at 375 nm, and for kaolin clay particles, $n = 1.55$–1.57.[19] These numbers ($n = 1.55$–1.57) are still different from $n = 1.62$ of polystyrene microbeads (enabling the maxima for polystyrene beads and silica/clay particles not to overlap with each other; see below), but are very close to it, potentially affecting the light scattering signals from microbead immunoagglutination assays. In the other filtration/concentration-based detection methods, however, the existence of such silica particles has been reported to be beneficial (and the interference from silica particles may be unavoidable). Feng *et al.*[20] reported that the use of pristine water (*i.e.* tap water) was not ideal in recovering oocysts from a sample. Rather, a sample matrix with silica in the 5–40 μm range with a turbidity of 5 NTU (nephelometric turbidity unit) yielded a high recovery rate of 85%, and 10 NTU yielded an even higher recovery rate of 91%.[20] Therefore, a method that will enable us to detect the immunoagglutination in the presence of such sample matrices (contaminants) should be suggested. We attempt to achieve this goal through utilizing Mie scatter theory.

Mie scatter theory has been described in great detail by others,[21] but will be briefly described here. Mie scatter is an angle dependent scatter technique in which the diameter of the particle causing the scatter is roughly equivalent to or much larger than the wavelength. Mie scatter assumes that a single particle can scatter from different points and that these different scattering centers can both constructively and destructively interfere with each other. This leads to an angular dependent, non-symmetric profile for scatter intensity. Mie light scatter intensities are given by eqn (1) and (2):

$$i_1 = \left| \sum_{n=1}^{\infty} \frac{2n+1}{n(n+1)} (a_n \pi_n \cos\theta + b_n \tau_n \cos\theta) \right|^2 \quad (1)$$

$$i_2 = \left| \sum_{n=1}^{\infty} \frac{2n+1}{n(n+1)} (a_n \tau_n \cos\theta + b_n \pi_n \cos\theta) \right|^2 \quad (2)$$

where i_1 and i_2 are the complex scattering amplitudes for two orthogonal directions of incident polarization. π_n and τ_n are angular dependent functions expressed in terms of Legendre polynomials. The coefficients a_n and b_n are given by eqn (3) and (4) respectively:

$$a_n = \frac{\psi_n(z)}{\zeta_n(z)} A_n \quad (3)$$

$$b_n = \frac{\psi_n(z)}{\zeta_n(z)} B_n \quad (4)$$

where A_n and B_n are quantities that depend on the ratios and logarithmic derivatives of the Riccati–Bessel functions, ζ_n and ψ_n. These are given by the following equations:

$$\zeta_n(z) = \sqrt{\frac{\pi z}{2}} \left[J_{n+1/2}(z) + i Y_{n+1/2}(z) \right] \quad (5)$$

$$\psi_n(z) = \sqrt{\frac{\pi z}{2}} J_{n+1/2}(z) \quad (6)$$

where $J_{n+1/2}(z)$ = the half-integer-order Bessel function of the first kind, $Y_{n+1/2}(z)$ = the half-integer-order Bessel function of the second kind, and $z = \pi d/\lambda$, the size parameter of the scattering particle.[21]

The angle dependence can be seen in Fig. 1, produced using Mie scatter calculation software.[22] Unlike Rayleigh scattering, the scatter intensity does not change monotonously against the angle; rather it "fluctuates", generating many "maxima". Through careful selection of light scattering parameters, namely the bead diameter (d) and the wavelength of incident light (λ), with the given refractive indices (n) of beads and sample matrix, it is possible to make such maxima for beads and for sample matrix not to overlap with each other, so that the Mie scatter detection can be made in the presence of a turbid sample matrix. Fig. 2 is an enlarged version of Fig. 1 for a narrower range of scatter angles (30° to 60°), considering: (1) the geometric limitations imposed on microfluidic channels (*i.e.* inability to separate incident and scattered light with 0°–30°

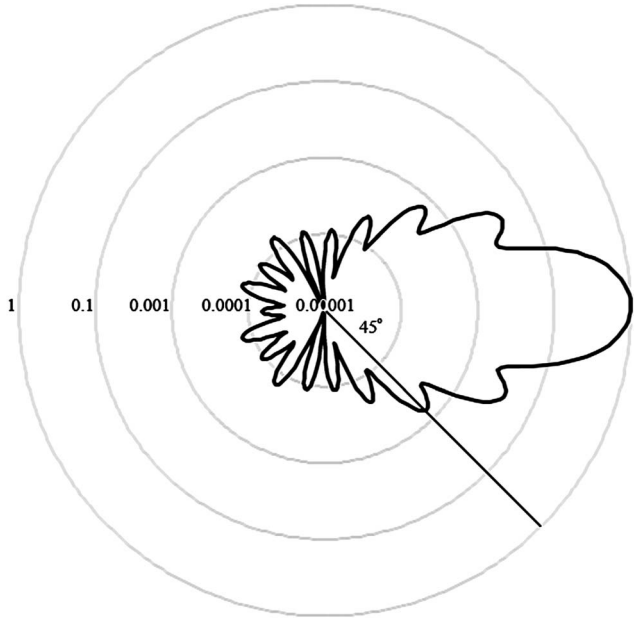

Fig. 1 Result of Mie scatter calculation on a polar-logarithmic plot. The line is at 45° where our scatter detections were made.

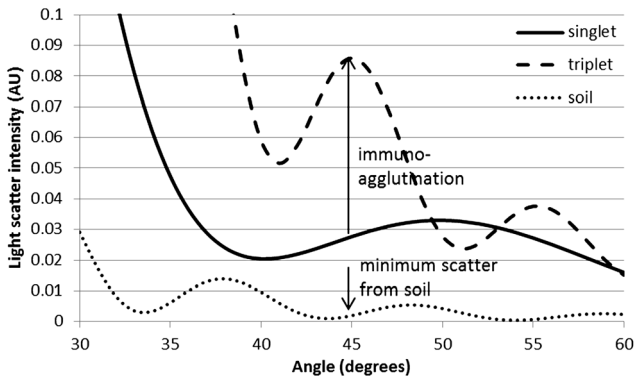

Fig. 2 Results of Mie scatter calculations (λ = 375 nm) for singlet microbeads (920 nm, n = 1.62, non-immunoagglutinated), triplet microbeads (immunoagglutinated), and silica particles (n = 1.56; d = 5 μm), showing at 45° the biggest change in Mie scatter intensity and the minimum background scatter from silica particles.

detection and inability to collect scatter signals with almost-parallel-to-channel 60°–90° detection) and (2) generally weaker signals with back scatter angles (90° to 180°). Through these calculations, it is possible to plot the scatter intensities for singlet (non-immunoagglutinated) and triplet (the most effectively immunoagglutinated) polystyrene beads (n = 1.62), and the silica particles (n = 1.56) within water (n = 1.34). Many different combinations of d and λ have been calculated, and the result shown in Fig. 2, with d = 920 nm and λ = 375 nm, provides the best results: at the scattering angle θ = 45°, the scattering from triplet beads is at the maximum, while that from silica particles is at the bottom valley. This allows for little noise in the signal due to particulate matter in the sample matrix.

Using these strategies, microfluidic detection with short sonication, and the Mie scatter optimization, we attempt to provide a field-deployable and near-real-time microfluidic biosensor for sensitive detection of *Cryptosporidium parvum*.

Materials and method

Sample preparation

Cryptosporidium parvum oocysts were purchased from the Sterling Parasitology Laboratory (The University of Arizona, Tucson, AZ, USA) at a concentration of 10^8 oocysts per mL. These were kept in a phosphate buffered saline (PBS) solution in a refrigerator at 4 °C. Serial dilutions were made to 10^5 oocysts per mL and this solution was sonicated for 4 minutes at 40 kHz using a Branson 2510 ultrasonic cleaner (Branson Ultrasonics, Danbury, CT, USA). This sonicated solution was serially diluted (5 dilutions were made) until a final concentration of 1 oocyst mL^{-1} (= 6 ng mL^{-1}) was reached.

Bradford assays were also performed for these solutions, according to the manufacturer's instructions (Bio-Rad Laboratories, Inc., Hercules, CA, USA; Bio-Rad Quick Start Assay 1×: 500-0205) with bovine serum albumin (Sigma-Aldrich Co., St. Louis, MO, USA; catalog number A7030) as a protein standard. Absorbance was measured using a Beckman 640 spectrophotometer (Beckman Coulter Inc., Brea, CA, USA) set at 595 nm. 1 oocyst per mL corresponded to 5.7 ng mL^{-1} proteins (antigens).

For the standard curve, the above serial dilutions of *Cryptosporidium* oocysts in PBS were used. The negative control was just sterile PBS. Field samples were collected from a chlorine treated swimming pool, and a sump at the University of Arizona Campus Agricultural Center. These samples were collected in sterile 50 mL centrifuge tubes (Fisher brand, Thermo Fisher Inc., Pittsburgh, PA, USA). These were then stored under refrigerated conditions at 4 °C. The pool sample was aliquoted into 2 mL tubes and treated with UV light for 30 minutes to reduce the chlorine content.[23]

The samples were spiked with *Cryptosporidium* oocysts (sonicated) using the above procedure, ranging in their final protein concentrations from 1 to 10^4 oocysts per mL (5.7 ng mL^{-1} to 57 μg mL^{-1}) with virtually no field sample dilution occurring. An unspiked aliquot of each field sample was used as a negative control for that field sample's data set.

Microbead preparation for the immunoagglutination assay was performed as described previously[21] for 920 nm beads, except using anti-*C. parvum* (Pierce Biotechnology, Rockford, IL, USA; catalog number PA173183) antibodies. Anti-*C. parvum* was covalently conjugated to 920 nm highly carboxylated polystyrene beads (Bangs Laboratories, Fishers, IN, USA). These beads, when covalently bound to the antibodies, were stable for up to one month after the conjugation process is completed.[24]

Testing device and conditions

Testing for all samples was performed using an LS-450 (Ocean Optics, Dunedin, FL, USA) UV light source peaking at 375 nm and a USB4000 miniature spectrometer (Ocean Optics) and SpectraSuite® software (Ocean Optics). The experimental apparatus is shown in Fig. 3. The plastic tray accommodating the microfluidic chip as well as the optical fibers (connected to the LS-450 and USB4000) was modeled in SolidWorks® (Dassault Systèmes SolidWorks Corporation, Waltham, MA, USA) and

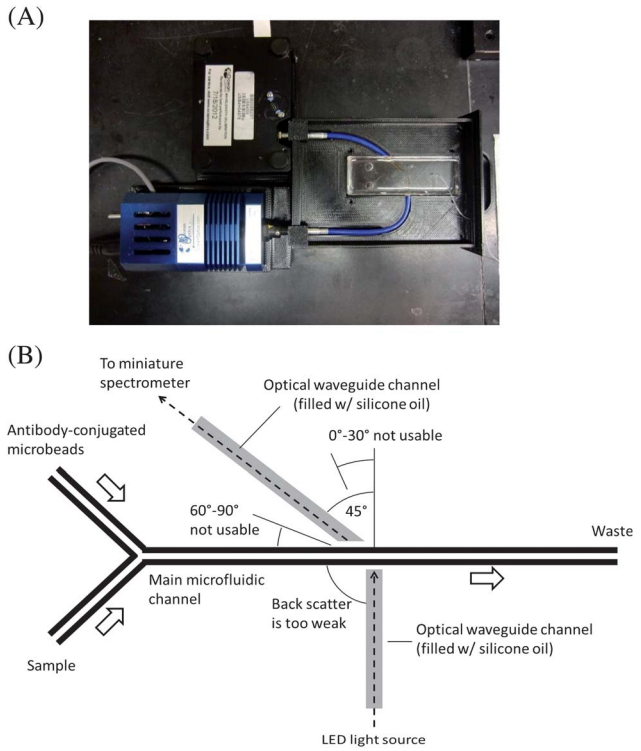

Fig. 3 (A) The experimental apparatus showing the light source (LS-450; lower left), microfluidic chip and tray (right), and the miniature spectrometer (USB4000; top left). (B) Schematic of the microfluidic chip used in the optical biosensor device. The end of the optical waveguide channel is separated by 100 μm from the sample channel in the middle. A syringe is connected to the outlet ("waste") to withdraw liquid from the sample channel with negative pressure.

manufactured using a Dimension uPrint® rapid prototyping device (Stratasys Inc., Eden Prairie, MN, USA) with acrylonitrile butadiene styrene (ABS) material (Stratasys Inc.). The microfluidic chips were made by a replica molding technique with polydimethylsiloxane (PDMS) from a silicon mold fabricated using deep reactive ion etching (DRIE). The microfluidic chip consisted of a y-channel for the sample and beads. The channel is 1 mm wide and 100 μm deep. The LS-450 was connected, *via* an optical fiber, to the waveguide channel at a 90° angle to the sample channel. This was filled with microscope immersion oil (mineral oil; with a refractive index of 1.515 at 23 °C). Another waveguide channel, at a 45° angle to the sample channel, was also filled with immersion oil and connected *via* an optical fiber to the USB4000. This configuration measures 45° forward Mie scatter that was calculated to yield maximum scatter intensity change for microbead immunoagglutination (Fig. 2).[15] Both waveguide channels were separated from the sample channel by 100 μm vertical wall of PDMS. A flat PDMS slide was then bonded to the molded chip using an oxygen plasma bake to permanently bond the two halves of the chip.[15]

After preparation, 15 μL of solution, beginning with the negative control and increasing in concentration to 10^4 oocysts per mL (= 57 μg mL^{-1}) were placed in the lower well sequentially (Fig. 3) and 15 μL of antibody-conjugated beads were placed in the top well. Both solutions were then drawn through the chip using negative pressure, created by an empty 250 μL syringe drawn out as slowly as possible through a tube connected to the end of the microfluidic channel. The sample was allowed to sit in the channel for one minute before a data point, averaging 5 scans every 50 ms, was collected at 375 nm from the SpectraSuite® software. Continuous data was also collected during this period every 5 ms. The maximum values were collected and normalized to the unspiked sample light scatter intensity value. This data collection process was repeated three times for each sample at each concentration (using different chips each time), including unspiked samples, and the normalized values were averaged such that the standard error could be found.

Chlorine analysis

N,*N*-Diethyl-*p*-phenylenediamine (DPD) was purchased from Thermo Scientific Orion (Thermo Scientific Orion, Thermo Fisher Inc., Pittsburgh, PA, USA) in the form of two powder chemistry packs.[25,26] One pack was for free chlorine (catalog number 13-642-220) and the other for total chlorine (catalog number 13-642-211). A standard was prepared using potassium permanganate ($KMNO_4$) purchased from Fisher Scientific (Fisher Brand, Thermo Fisher Inc., Pittsburgh, PA, USA; catalog number AC42417-0250). 10 mL dilutions of $KMNO_4$ were made in the range of 0.5–3.0 ppm chlorine equivalent concentrations. DPD powder packs were added to these standard solutions and field water samples, as well as deionized water as a blank, and mixed well immediately prior to measuring absorbance at 515 nm using a Beckman 640 spectrophotometer. A standard curve was constructed through second-order polynomial regression using Microsoft Excel® and used to identify the free and total chlorine concentrations of field water samples, specifically from a chlorinated swimming pool before and after UV treatment.

Bacterial culture

All water samples, including PBS, were cultured to identify the existence of any bacterial contaminants, in sterile agar plates from BD Diagnostic Systems (Thermo Fisher Inc., Pittsburgh, PA, USA; catalog number L21934) using 0.5 mL of sample and spread in a circular manner about the plate with a sterilized wand. They were cultured in the dark at 37 °C overnight and counted.

Cross-reactivity test with *E. coli* K12

The cross-reactivity of anti-*C. parvum* conjugated beads was tested using *Escherichia coli* K12, cultured overnight at 37 °C in a flask of brain heart infusion. This stock solution was serially diluted to 10^{-2} to 10^{-8}. These dilutions were plated (0.5 mL each) in sterile agars, as described above, and the number of colonies was counted to assess the colony forming units (CFU). After plating, the remaining solution was sonicated as described above. Microbead immunoagglutination assays were performed for these *E. coli* K12 solutions using anti-*C. parvum* conjugated beads in an optical microfluidic biosensor system as described above.

Results

Microscopic observations

Fig. 4 shows the 40× microscope images of oocysts in PBS (top left); oocysts sonicated for 4 minutes in PBS (bottom left); the anti-*C. parvum* conjugated beads with oocysts in PBS (top right); and anti-*C. parvum* conjugated beads with sonicated oocysts in PBS (bottom right). For all four cases, the *C. parvum* concentrations were 10^6 oocysts per mL (5.7 mg mL^{-1}). Oocysts are larger black ovals, while beads are smaller spheroid dots. Large asymmetrical shapes represent agglutination. There are a greater number of oocysts shown in the non-sonicated image while the sonicated oocysts show higher rates of agglutination as well as a larger size of agglutinated beads. This indicates that the extent of immunoagglutination increases upon sonication of oocysts.

Standard curve

A standard curve was created using *Cryptosporidium parvum* oocysts in PBS. The scatter intensity measurements varied from chip to chip (due to the variance in optical characteristics and channel geometry), therefore it was necessary to normalize all measurements with those of "negative controls", (*i.e.*, the measurement of zero oocyst concentration) taken immediately prior to spiked sample measurements. The results show a mostly increasing response from the negative control to the final concentration of 10^4 oocysts per mL (= 57 μg mL^{-1}) (Fig. 5). All points, except the 1 oocyst per mL (= 5.7 ng mL^{-1}) concentration, were found to be significantly different from the negative control. Therefore, the detection limit of this assay is 10 oocysts per mL (without any filtration or concentration). Given the volume of the sample introduced to a microfluidic biosensor, 15 μL, this is actually sub-single-oocyst-level detection per sample. With proper filtration/concentration, this method should be able to detect ≤1oocyst per large volume of water (*e.g.*, 10 L), comparable to or better than that of EPA Method 1623. This can easily be explained by the fact that the sample was sonicated in a larger volume with a higher concentration, thus antigens (COWP) were liberated, and an aliquot was made from it. They gave a scatter intensity change up to approximately 15% and an average standard error of 2.0%.

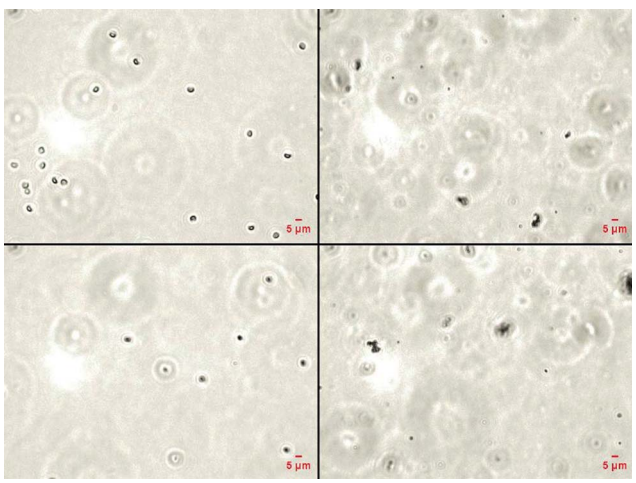

Fig. 4 All images shown at 40× magnification using 10^6 oocysts per mL with a scale bar representing 5 μm. Top left: *Cryptosporidium parvum* oocysts in PBS. Bottom left: oocysts after four minutes of sonication in PBS. Top right: oocysts agglutinated with antibody-conjugated beads. Bottom right: oocysts sonicated for four minutes and agglutinated with antibody-conjugated beads. Oocysts are larger black ovals, while beads are smaller spheroid dots. Large asymmetrical shapes represent agglutination. There are a greater number of oocysts shown in the non-sonicated image while the sonicated oocysts show higher rates of agglutination as well as larger agglutinated beads.

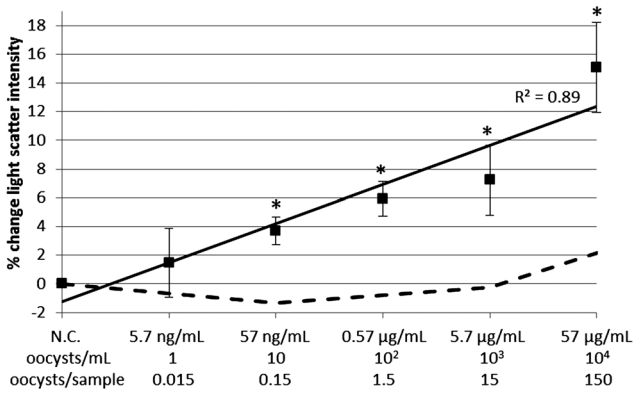

Fig. 5 Standard curve with oocyst-spiked PBS after four minutes of sonication (solid line), shown together with the cross-reactivity result (dashed line) for *E. coli* K12 (in CFU mL^{-1} unit) using anti-*C. parvum* conjugated beads.

To test the cross-reactivity of anti-*C. parvum* conjugated beads, *E. coli* K12 was cultured and serially diluted. 10^{-6} dilution showed a concentration of 10^3 CFU mL^{-1} with agar plate counting. 10^{-4} to 10^{-8} dilutions (corresponding to 10^5 to 10^1 CFU mL^{-1}, respectively), as well as PBS as a negative control, were tested using anti-*C. parvum* conjugated beads with microfluidic immunoagglutination assays as described above. This result is shown as a dashed line in Fig. 5, while the unit is CFU mL^{-1}, not oocysts per mL. The scatter intensity change does not go beyond 2%, which is smaller than the average standard error (2.0%) of the standard curve, indicating that *E. coli* K12 did not cross-react with anti-*C. parvum* conjugated beads.

Swimming pool sample

Swimming pool water tests show a signal intensity change up to approximately 11% (Fig. 6). The average standard error is 2.5%, higher than 2.0% of the standard curve. Again all measurements were normalized with those of negative controls using the same field water sample as described above. All data points, except the 1 oocyst per mL (= 5.7 ng mL^{-1}) concentration, were found to be significantly different from the negative control (unspiked sample). The detection limit is again 10 oocysts per mL (= 57 ng mL^{-1}) without filtration/concentration, or ≤1 oocyst per sample with filtration/concentration.

The result shown in Fig. 6 (solid line) was obtained after the UV treatment to pool water as described. Initially, this experiment was performed without UV irradiation, but no noticeable scatter intensity change could be found (shown as a dashed line in Fig. 6. The pool water represents a chemically active, but largely biologically inactive sample as shown by bacterial culture and chlorine analysis.

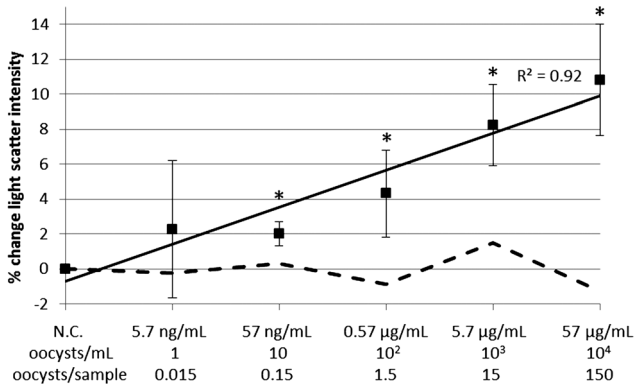

Fig. 6 Assay results with oocyst-spiked swimming pool water after four minutes of sonication, with UV treatment (solid line) or without UV treatment (dashed line).

The pool water was plated in agar and cultured overnight at 37 °C. There was no growth on the plate, indicating non-existence of bacterial contamination. The pool water was also tested for its free and total chlorine concentrations. Two standard curves were generated and the free and total chlorine concentrations after UV treatment were estimated to be 0.631 ± 0.004 ppm (free chlorine) and 0.52 ± 0.02 ppm (total chlorine). These two values are nearly identical to each other, indicating most chlorine in the swimming pool water was free chlorine. In addition, these values are substantially lower than those of untreated swimming pool water, 2–5 ppm, indicating successful removal of chlorine from the water sample.

Sump water sample

Water collected from the University of Arizona Campus Agricultural Center sump shows just less than a 7% change in light scatter intensity from the negative control to the maximum concentration of 10^4 oocysts per mL (= 57 µg mL^{-1}) (Fig. 7). All data points in this set are significantly different from the negative control. Detection limit of this assay is 1 oocyst per mL (= 5.7 ng mL^{-1}) without filtration/concentration or ≤1 oocyst per sample with filtration/concentration. This is still possible since antigens were liberated and 15 µL aliquots were made from it

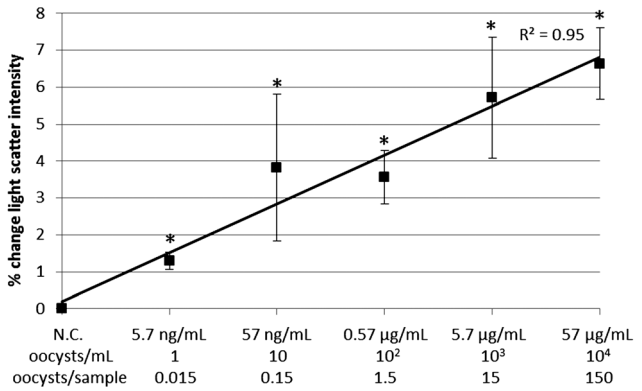

Fig. 7 Assay results with oocyst-spiked sump water after four minutes of sonication. This water sample contains bacteria and soil particles, as well as other contaminants.

prior to experiments. The 7% intensity change for sump water is substantially smaller than those of the standard curve (15%) and pool water (11%), indicating a lesser extent of immunoagglutination. This was a more turbid sample and likely more representative of water collected from a river. Turbid water has been shown to cause assay problems in the past.[27]

The average standard error was much smaller (1.1%) than 2.0% of a standard curve and 2.5% with sump water. (Note that the size of error bars may look similar to those of a standard curve and with sump water, but it is much smaller due to the smaller scale of the *y*-axis.)

The sump water culture resulted in a concentration of 70 CFU mL^{-1} after overnight culture in agar at 37 °C. The chlorine content was not significant and thus no UV treatment was necessary.

Discussion

Detection sensitivity

The samples tested, including all field samples, showed positive readings for most *C. parvum* concentrations. Agglutination was confirmed using a light microscope as shown in Fig. 3. Even though the percent intensity change was different by the type of field water sample, the shape of the curve produced was very similar across all samples. The curve intensity changes were nearly all significantly different from their respective negative control, showing that this testing method was reliable. Without filtration/concentration, this method can be used as a faster, near-real-time assay with the total assay time of 10 min including the 4 min sonication time and the detection limit of 10 oocysts per mL (= 57 ng mL^{-1} antigens) for the PBS and swimming pool samples and 1 oocyst per mL (= 5.7 ng mL^{-1} antigens) for the sump water sample. When combined with filtration/concentration, this method is able to detect the required ≤1 oocyst per 10 L water sample, comparable to or potentially better than the EPA Method 1623, while effectively reducing the time and labor necessary for staining and microscopic analysis.

Effects of contaminants

The differences in intensity change indicate that there was a contaminant, or possibly multiple contaminants, in the field sample matrices that were affecting immunoagglutination. The ability to detect differences in concentration of *C. parvum* oocysts was maintained in all field samples.

The pool sample had significant amounts of chlorine. When this was reduced using UV light treatment, it was clear that we were able to detect the oocysts. This is because the antibodies were quickly denaturing in the chlorinated water, since chlorine existed as hypochlorite (*i.e.* bleach) that has been known to denature most proteins. When the water was treated with UV light, however, the reduction in chlorine content was great enough to allow for immunoagglutination.

The sump sample was un-chlorinated, but biological material (bacteria) and sediment (soil particles) were found to be in the sample. Tests with *E. coli* K12 showed that the anti-*C. parvum* conjugated beads were not likely cross-reacting with other bacteria in the sample.

Table 2 Raw scatter intensities of field water samples without spiking oocysts (first row = turbidity) and plus anti-*C. parvum* conjugated beads (second row = negative control), shown together with the maximum scatter intensity changes of each *C. parvum* assay (third row)[a]

	PBS	Pool	Sump
Turbidity	3780 ± 50	3830 ± 20	3810 ± 30
Negative control	2750 ± 110	3140 ± 30	3410 ± 160
Maximum intensity change	15%	11%	6.5%

[a] Note: all data are shown with standard errors. Turbidity and negative controls are not directly comparable to each other, since a different set of optical fibers were used for turbidity measurement.

To explain the different scatter intensity changes of all water samples, we examined the raw scatter intensities of all negative controls (zero oocyst spiked water sample + anti-*C. parvum* conjugated beads) (Table 2). Due to chip-to-chip variations (this is the reason why all scatter intensities were normalized to those of negative controls taken immediately prior to each assay), the standard errors of these raw intensities were large. However, there is a clear difference over the water samples, in the order of sump (3410) > pool (3140) > PBS (2750). The maximum scatter intensity change was also in the order of sump (6.5%) < pool (11%) < PBS (15%). It is clear that the larger scatter intensity for a negative control is related to a smaller extent of scatter intensity change. Chlorine, inorganic matter (soil particles), organic matter (fecal matter and proteins), and bacteria, negatively influence the extent of immunoagglutination. It is possible these inorganic and organic matters affected the stability of the antibody-conjugated beads, resulting in non-specific aggregation, and thus reducing the number of available antibody-conjugated beads that could immunoagglutinate.

One other possible explanation is the difference in turbidity among the water samples, which may affect the scatter intensity measurements. Therefore, we measured the raw scatter intensities of just the water samples (no beads) using the microfluidic system. The raw scatter intensities were (shown in Table 2 with standard errors): sump (3810), pool (3830) and PBS (3780), showing no significant differences among water samples. This is analogous to Fig. 2, where the scatter detection at 45° with 375 nm light would minimize the background scatter from the silica particles. Therefore, the turbidity effect can be duly ruled out.

Therefore, the smaller scatter intensity change can be correlated with the existence of contaminants in the water sample that reduced the number of available antibody-conjugated beads. However, this does not explain why the detection limit is lower for the sump water (1 oocyst per mL = 5.7 ng mL^{-1} antigens). Obviously, the lower detection limit was attributed to the smaller error bars (2.0% for PBS, 2.5% for pool water and 1.1% for sump water), *i.e.* the scatter intensity changes were more reproducible with sump water. In the previous paragraph, we concluded that such contaminants triggered some non-specific aggregation of beads and reduced the number of available antibody-conjugated beads that could immunoagglutinate. Perhaps this was an effective way to eliminate unstable beads so that more reproducible results could be obtained. Some portion of the contaminants might act as surfactants to further stabilize the beads.

Additionally, we described in the introduction that the use of turbid water (with 5–40 μm silica particles with 5–10 NTU) yielded better recovery of oocysts during filtration/concentration and better assay results.[20] The existence of silica particles in the water sample is perhaps required to effectively eliminate non-stable components and improve the reproducibility of the assay.

Conclusion

It is clear that field samples can be quickly, easily, and accurately tested for *Cryptosporidium parvum* oocysts. Our detection limit is reasonably lower than many other previous attempts (see Table 1) at the sub-single-oocyst-level considering the small sample size. The assay required neither substantial labor nor trained technicians. Simple pre-treatments such as UV treatment and/or sonication were necessary, but it is potentially practiced in field setting. This method can be used in two different settings: (1) use without any filtration/concentration, as a near-real-time (<10 min) assay with the detection limit of 1–10 oocysts per mL, and (2) use with filtration/concentration, as an improvement to the other methods (especially EPA Method 1623, replacing its staining and microscopic analysis), with the sub-oocyst-level detection limit.

Acknowledgements

Funding for this work was provided by Animal, Plant and Fisheries Quarantine and Inspection Agency (QIA), South Korea, award number C-AD14-2006-11-0. S.V.A. also acknowledges the fellowship support from Water Sustainability Program (WSP) of the University of Arizona.

References

1 U.S. Environmental Protection Agency (EPA), *National Primary Drinking Water Regulations: Long Term 2 Enhanced Surface Water Treatment Rule*, http://water.epa.gov/lawsregs/rulesregs/sdwa/lt2/index.cfm, 2006.
2 R. Fayer, *Vet. Parasitol.*, 2004, **126**, 37–56.
3 C. L. Chappell, P. C. Okhuysen, R. Langer-Curry, G. Widmer, D. E. Akiyoshi, S. Tanriverdi and S. Tzipori, *Am. J. Trop. Med. Hyg.*, 2006, **75**, 851–857.
4 K. J. Ryan and C. G. Ray, *Sherris Medical Microbiology: An Introduction to Infectious Disease*, McGraw-Hill, New York, 4th edn, 2004.
5 J. B. Rose, *Annu. Rev. Public Health*, 1997, **18**, 135–161.
6 J. A. Castro-Hermida, I. García-Presedo, A. Almeida, M. González-Warleta, J. M. C. Da Costa and M. Mezo, *Water Res.*, 2009, **43**, 4133–4142.
7 R. Fayer, U. Morgan and S. J. Upton, *Int. J. Parasitol.*, 2000, **30**, 1305–1322.
8 J. A. Castro-Hermida, I. García-Presedo, A. Almeida, M. González-Warleta, J. M. Correia Da Costa and M. Mezo, *Sci. Total Environ.*, 2008, **405**, 45–53.
9 D. G. Korich, J. R. Mead, M. S. Madore, N. A. Sinclair and C. R. Sterling, *Appl. Environ. Microbiol.*, 1990, **56**, 1423–1428.
10 G. F. Craun, J. M. Brunkard, J. S. Yoder, V. A. Roberts, J. Carpenter, T. Wade, R. L. Calderon, J. M. Roberts, M. J. Beach and S. L. Roy, *Clin. Microbiol. Rev.*, 2010, **23**, 507–528.
11 United States Environmental Protection Agency (EPA), *Method 1623:* Cryptosporidium *and* Giardia *in Water by Filtration/IMS/FA*, http://www.epa.gov/microbes/documents/1623de05.pdf, 2005.
12 J. A. Castro-Hermida, I. García-Presedo, A. Almeida, M. González-Warleta, J. M. Correia Da Costa and M. Mezo, *Water Res.*, 2008, **42**, 3528–3538.
13 A. R. Jex and R. B. Gasser, *Biotechnol. Adv.*, 2010, **28**, 17–26.

14 J. L. Cantera, W. Chen and M. V. Yates, *Appl. Environ. Microbiol.*, 2010, **76**, 584–588.
15 B. C. Heinze, J. R. Gamboa, K. Kim, J.-Y. Song and J.-Y. Yoon, *Anal. Bioanal. Chem.*, 2010, **398**, 2693–2700.
16 D. J. You, K. J. Geshell and J.-Y. Yoon, *Biosens. Bioelectron.*, 2011, **28**, 399–406.
17 M. Inoue, S. Uga, T. Oda, S. K. Rai, G. Vesey and H. Hotta, *Water Res.*, 2006, **40**, 881–886.
18 I. Oyane, M. Furuta, C. E. Stavarache, K. Hashiba, S. Mukai, J. M. Nakanishi, I. Kimata and Y. Maeda, *Environ. Sci. Technol.*, 2005, **39**, 7294–7298.
19 (*a*) M. Polyanskiy, Refractive Index Database, http://refractiveindex.info, 2011; (*b*) S. N. Kasarova, N. G. Sultanova, C. D. Ivanov and I. D. Nikolov, *Opt. Mater.*, 2007, **29**, 1481–1490; (*c*) G. Ghosh, *Opt. Commun.*, 1999, **163**, 95–102; (*d*) P. Weidler and F. Friedrich, *Am. Mineral.*, 2007, **92**, 1130–1132.
20 Y. Y. Feng, S. L. Ong, J. Y. Hu, L. F. Song, X. L. Tan and W. J. Ng, *Appl. Environ. Microbiol.*, 2003, **69**, 1898–1903.
21 B. C. Heinze and J.-Y. Yoon, *Colloids Surf., B*, 2011, **85**, 168–173.
22 S. Prahl, Mie Scattering Calculator, http://omlc.ogi.edu/calc/mie_calc.html, 2012.
23 L. H. Nowell and J. Hoigné, *Water Res.*, 1992, **26**, 593–598.
24 H.-J. Kwon, Z. S. Dean, S. V. Angus and J.-Y. Yoon, *JALA*, 2010, **15**, 216–223.
25 Thermo Orion Scientific, Free chlorine DPD method AC4P71, Thermo Fisher Scientific, 2003.
26 Thermo Orion Scientific, Low-range total chlorine Method AC2072, Thermo Fisher Scientific, 2002.
27 L.-A. H. Krometis, G. W. Characklis and M. D. Sobsey, *Appl. Environ. Microbiol.*, 2009, **75**, 6619–6621.
28 J. Quílez, C. Sánchez-Acedo, A. Clavel, E. del Cacho and F. López-Bernad, *Vet. Parasitol.*, 1996, **67**, 75–81.
29 L. S. Garcia, T. C. Brewer and D. A. Bruckner, *J. Clin. Microbiol.*, 1987, **25**, 119–121.
30 S. A. Henriksen and J. F. Pohlenz, *Acta Vet. Scand.*, 1981, **22**, 594–596.
31 M. J. Arrowood and C. R. Sterling, *J. Clin. Microbiol.*, 1989, **27**, 1490–1495.
32 H. H. Stibbs and J. E. Ongerth, *J. Clin. Microbiol.*, 1986, **24**, 517–522.
33 S. Pohjola, L. Jokipii and A. M. M. Jokipii, *Vet. Rec.*, 1985, **115**, 442–443.
34 G. Vesey, J. S. Slade and C. R. Fricker, *Lett. Appl. Microbiol.*, 1991, **13**, 62–65.
35 G. Vesey, P. Hutton, A. Champion, N. Ashbolt, K. L. Williams, A. Warton and D. Veal, *Cytometry*, 1994, **16**, 1–6.
36 L. M. Valdez, H. A. N. Dang and P. C. Okhuysen, *J. Clin. Microbiol.*, 1997, **35**, 2013–2017.
37 D. J. Cole, K. Snowden, N. D. Cohen and R. Smith, *J. Clin. Microbiol.*, 1999, **37**, 457–460.
38 M. L. Power, S. R. Shanker, N. C. Sangster and D. A. Veal, *Vet. Parasitol.*, 2003, **112**, 21–31.
39 K. Kehl, H. Cicirello and P. L. Havens, *J. Clin. Microbiol.*, 1995, **33**, 416–419.
40 P. Ma and R. Soave, *J. Infect. Dis.*, 1983, **147**, 824–828.
41 G. Chichino, A. Bruno, C. Cevini, C. Atzori, S. Gatti and M. Scaglia, *J. Protozool.*, 1991, **38**, 212S–214S.
42 A. Elliot, U. M. Morgan and R. C. A. Thompson, *J. Gen. Appl. Microbiol.*, 1999, **45**, 139–142.
43 H. V. Smith, A. McDiarmid, A. L. Smith, A. R. Hinson and R. A. Gilmour, *Parasitology*, 1989, **99**(Pt 3), 323–327.
44 D. Baxby, N. Blundell and C. A. Hart, *J. Hyg.*, 1984, **93**, 317–323.
45 D. Moodley, T. F. Jackson, V. Gathiram and J. van den Ende, *SAMJ*, 1991, **79**, 314–317.
46 K. L. Rule and P. J. Vikesland, *Environ. Sci. Technol.*, 2009, **43**, 1147–1152.
47 M. C. Jenkins, C. N. O'Brien and J. M. Trout, *J. Parasitol.*, 2008, **94**, 94–98.
48 K. Z. Anusz, P. H. Mason, M. W. Riggs and L. E. Perryman, *J. Clin. Microbiol.*, 1990, **28**, 2770–2774.
49 B. L. Ungar, *J. Clin. Microbiol.*, 1990, **28**, 2491–2496.
50 C. A. Siddons, P. A. Chapman and B. A. Rush, *J. Clin. Pathol.*, 1992, **45**, 479–482.
51 J. Rosenblatt and L. Sloan, *J. Clin. Microbiol.*, 1993, **31**, 1468–1471.
52 G. A. Grigoriew, S. Walmsley, L. Law, S. L. Chee, J. Yang, J. Keystone and M. Krajden, *Diagn. Microbiol. Infect. Dis.*, 1994, **19**, 89–91.
53 R. Dagan, D. Fraser, J. El-On, I. Kassis, R. Deckelbaum and S. Turner, *Am. J. Trop. Med. Hyg.*, 1995, **52**, 134–138.
54 L. S. Garcia and R. Y. Shimizu, *J. Clin. Microbiol.*, 1997, **35**, 1526–1529.
55 C. R. Sterling and M. J. Arrowood, *Pediatr. Infect. Dis.*, 1986, **5**, S139–S142.
56 J. Rusnak, T. L. Hadfield, M. M. Rhodes and J. K. Gaines, *J. Clin. Microbiol.*, 1989, **27**, 1135–1136.
57 L. Xiao, R. P. Herd and D. M. Rings, *Vet. Parasitol.*, 1993, **47**, 17–23.
58 R. Chan, J. Chen, M. K. York, N. Setijono, R. L. Kaplan, F. Graham and H. B. Tanowitz, *J. Clin. Microbiol.*, 2000, **38**, 393–394.
59 W. Quintero-Betancourt, A. Gennaccaro and J. B. Rose, *Appl. Environ. Microbiol.*, 2003, **69**, 5380–5388.
60 C. L. Digiorgio, D. A. Gonzalez and C. C. Huitt, *Appl. Environ. Microbiol.*, 2002, **68**, 5952–5955.
61 D. S. Francy, O. D. Simmons, M. W. Ware, E. J. Granger, M. D. Sobsey and F. W. Schaefer, *Appl. Environ. Microbiol.*, 2004, **70**, 4118–4128.
62 M. LeChevallier, G. D. Giovanni, J. L. Clancy, Z. Bukhari, S. Bukhari, J. S. Rosen, J. Sobrinho and M. M. Frey, *Appl. Environ. Microbiol.*, 2003, **69**, 971–979.
63 J. A. Higgins, J. M. Trout, R. Fayer, D. Shelton and M. C. Jenkins, *Water Res.*, 2003, **37**, 3551–3560.
64 E. Kuczynska, D. G. Boyer and D. R. Shelton, *J. Microbiol. Methods*, 2003, **53**, 17–26.
65 S. Pohjola, E. Neuvonen, A. Niskanen and A. Rantama, *Acta Vet. Scand.*, 1986, **27**, 71–79.
66 M. Farrington, S. Winters, C. Walker, R. Miller and D. Rubenstein, *J. Clin. Microbiol.*, 1994, **32**, 2755–2760.
67 L. S. Garcia and R. Y. Shimizu, *J. Clin. Microbiol.*, 2000, **38**, 1267–1268.
68 M. J. Blears, N. J. Pokorny, R. A. Carreno, S. Chen, A. Stephanie, D. Grandis, H. Lee and J. T. Trevors, *J. Parasitol.*, 2000, **86**, 838–841.
69 T. K. Graczyk, E. J. Lewis, G. Glass, A. J. Dasilva, L. Tamang, A. S. Girouard and F. C. Curriero, *Parasitol. Res.*, 2007, **100**, 247–253.
70 M. Bednarska, A. Bajer, E. Sinski, A. S. Girouard, L. Tamang and T. K. Graczyk, *Parasitol. Res.*, 2007, **100**, 455–460.
71 U. Morgan, L. Pallant and B. Dwyer, *J. Clin. Microbiol.*, 1998, **36**, 995–999.
72 A. Wiedenmann, P. Kruger and K. Botzenhart, *J. Ind. Microbiol. Biotechnol.*, 1998, **21**, 150–166.
73 E. Chung, J. E. Aldom, A. H. Chagla, M. Kostrzynska, H. Lee, G. Palmateer, J. T. Trevors, S. Unger and S. De Grandis, *J. Microbiol. Methods*, 1998, **33**, 171–180.
74 C. L. Gibbons, F. M. Rigi and F. M. Awad-EI-Kariem, *Protist*, 1998, **149**, 127–134.
75 U. M. Morgan and R. C. Thompson, *Parasitol. Today*, 1998, **14**, 241–245.
76 H. V. Smith and R. A. B. Nichols, *Exp. Parasitol.*, 2010, **124**, 61–79.
77 T. D. Morse, R. A. B. Nichols, A. M. Grimason, B. M. Campbell, K. C. Tembo and H. V. Smith, *Epidemiol. Infect.*, 2007, **135**, 1307–1315.
78 Z. Misic and N. Abe, *Parasitology*, 2007, **134**, 351–358.
79 A. Bonnin, M. N. Fourmaux, J. F. Dubremetz, R. G. Nelson, P. Gobet, G. Harly, M. Buisson, D. Puygauthier-Toubas, G. Gabriel-Pospisil, M. Naciri and P. Camerlynck, *FEMS Microbiol. Lett.*, 1996, **137**, 207–211.

